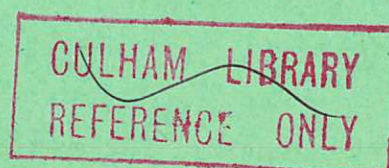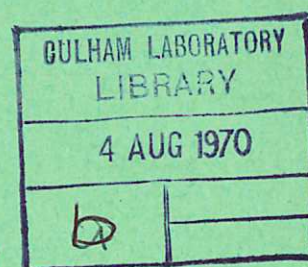United Kingdom Atomic Energy Authority

RESEARCH GROUP

Preprint

EXPERIMENTAL OBSERVATION OF THE DRIFT DISSIPATIVE INSTABILITY IN AN AFTERGLOW PLASMA

M. W. ALCOCK
B. E. KEEN

Culham Laboratory
Abingdon Berkshire

1970

EXPERIMENTAL OBSERVATION OF THE DRIFT DISSIPATIVE INSTABILITY IN AN AFTERGLOW PLASMA

by

M.W. ALCOCK
B.E. KEEN

A B S T R A C T

Measurements are reported on low frequency self-excited oscillations in an inhomogeneous afterglow plasma, in which there is a radial density gradient perpendicular to an axial homogeneous magnetic field. The plasma was produced either by using a short pulse of electrons emitted from a hot cathode to ionize the background gas, or by pulsing off an RF discharge. The plasma so formed had an initial density of $\sim 10^{10}$ cm^{-3} and a temperature $T_e \sim 1000^{\circ}$K. The experiment was carried out using tubes of 2·5 and 5·0 cm diameter, giving inverse density scale lengths for the radial density gradient of $\sim 2·3$ and $\sim 1·3$ cm^{-1} respectively. The oscillations occurred mainly as $m = +1$ azimuthal modes although some results for $m = +2$ were obtained. The oscillations were shown to be standing waves in the axial direction z with a wavelength approximately λ_z, equal to the column length. It was found that the frequency of oscillation ω was dependent on column length and by varying this a dispersion relationship ω against $k_z = (2\pi/\lambda_z)$ could be plotted under various conditions. It was found that the frequency was independent of time (or density) in the afterglow and that the frequency of oscillation tended to zero as $k_z \to 0$ and to ω^* as k_z assumed larger values.

The simple theory of drift dissipative instabilities has been extended to include effects due to electron-neutral and ion neutral collisions and the $\text{Re}(\omega)$, and growth rates $\text{Im}(\omega)$, against k_z have been calculated for the relevant experimental cases. Comparison of theory and experiment shows remarkably good agreement considering the possible errors in some of the experimental quantities and the assumptions present in the theory.

U.K.A.E.A. Research Group,
Culham Laboratory,
Abingdon,
Berks

February, 1970

C O N T E N T S

1. INTRODUCTION

During the last few years there has been much interest in the low frequency oscillations or instabilities occurring in inhomogeneous magneto-plasmas. This is due to the possible anomalous cross-field diffusion caused by the presence of these micro-instabilities. Of particular interest are those instabilities occurring in a plasma with a density gradient perpendicular to the containing magnetic field, in the cases where collisions between particles or lack of collisions may lead to oscillations. These self sustained oscillations are the so-called 'drift instabilities', and their main properties in both the collisional and collisionless regimes have been summarized by Kadomtsev[1] and Mikhailovski[2]. Unfortunately, in most experiments on drift waves which have been reported radial electric fields as well as radial density gradients have existed in the plasma. The electric field together with the longitudinal magnetic field leads to an azimuthal rotation of the plasma, and consequently, causes a Doppler shift of the instability frequency[3-6]. Further, it has been shown[7] that in an inhomogeneous plasma a rotationally convected drift-type instability can be supported if collisions exist in the presence of this radial electric field.

In afterglow plasmas, however, the radial electric field is absent, as are the other possible causes of instabilities such as axial current, non-isotropic velocity distributions, and imposed electric fields. Consequently, most experiments on afterglows had shown them to be stable, but recently Pigache and Harding[8] have reported the observation of drift-waves in a helium afterglow. This paper reports futher results obtained in both helium and hydrogen afterglow plasmas, on a low frequency instability. Experiments have

been performed in two different tubes, thus varying the density gradient scale length, and in different axial magnetic fields. The instability frequency was measured as the axial wavelength was varied in each case, and this allowed a dispersion diagram to be constructed. Further measurements were made using a microwave cavity technique[9,10] to determine the electron-neutral collision frequency.

Sec.2 develops the theory of the drift-dissipative instability[11,12] in which both ion-neutral and electron neutral collisions are included. Sec.3 discusses the apparatus and the diagnostic techniques used to determine the DC properties and the instability characteristics of the plasma. The results obtained using these methods are reported in Sec.4, and Sec.5 compares the results with the foregoing theoretical predictions. Finally, it is concluded that good agreement is obtained between the simple theory of the drift dissipative instability and the experimental results, in view of experimental errors and the approximations in the theory.

2. THEORY

There have been a number of papers recently, which have considered the problem of collisional drift waves in a magneto-plasma. Notable among these was that of Hendel, Chu and Politzer[5] who achieved a considerable amount of success in applying their linearized theory to the experimental results. In their particular case, the theory was mainly applicable to a fully ionized plasma in which the important collisions for instability were the ion-electron collisions, whereas the stabilizing influence came from finite ion-Larmor radius effects and ion-ion collisions. However, in the afterglow plasma considered here, the important collisional times are those concerned with electron-neutral and ion-neutral collisions. A theory of the stability

of a gas discharge in a magnetic field with no longitudinal current

in the plasma has been developed by Timofeev[11,12] and Kadomtsev[1].

They have described the plasma behaviour by the equations of

continuity for the electrons and ions, together with the equations

of motion for each of these species. Low frequency oscillations were

considered under the conditions that the plasma was neutral, and thus

the ion and electron densities were equal. The equations of continuity

were, then:

$$\frac{\partial n_i}{\partial t} + \overline{\nabla} \cdot (n\overline{v}_i) = 0$$

$$\frac{\partial n_e}{\partial t} + \overline{\nabla} \cdot (n\overline{v}_e) = 0 \tag{1}$$

The velocities of the electrons and ions, $\overline{v}_e$, and $\overline{v}_i$ were found

from the equations of motion, in which the electrons were assumed to

be inertialess, but the ion motion takes into account inertia and

collisions with neutrals. The non-isothermal case $T_e \gg T_i$ was con-

sidered, and thus ion pressure was neglected, resulting in the follow-

ing equations of motion:

$$- T_e \frac{\overline{\nabla} n_e}{n_e} + e\overline{\nabla}\varphi - \frac{e}{c}[\overline{v}_e \wedge \overline{H}] - m\overline{v}_e \, \nu_e = 0 \tag{2}$$

$$M_i \frac{d\nu_i}{dt} = - e\overline{\nabla}\varphi + \frac{e}{c}[\overline{v}_i \wedge \overline{H}] - M_i\overline{v}_i\nu_i = 0 \tag{3}$$

Here H is the magnetic field, φ the electric potential,

$n_i = n_e = n$ the density, ν_i and ν_e, the ion and electron colli-

sion frequencies with neutrals respectively, and M_i and m the

corresponding masses of ions and electrons.

The above equations were solved under the following approximations:

(i) The slab model was adopted in the localized approximation.

(ii) The equations were linearized to first-order for small perturba-

tions of density n, and potential φ_1, in which the perturba-

tion was taken in the form $\exp - i(\omega t + \overline{k} \cdot \overline{r})$. Here, ω is the

- 3 -

oscillation frequency, and $\bar{k}$ is the wave-vector.

(iii) The calculation was considered in the case of oblique propagation to the magnetic field H in which it was assumed that $k_y \gg k_x \gg \frac{1}{n_0}\left(\frac{dn_0}{dx}\right)$. Here H was taken to be uniform in the z direction, while the density gradient was assumed to be along the x direction.

(iv) The low frequency approximation was considered in which the oscillation frequency $\omega \ll \Omega_i (\Omega_i = \frac{eH}{M_i c}$, the ion cyclotron frequency).

(v) It was assumed that there were no zero order electric fields present in the plasma (i.e. $\nabla\varphi_0 = 0$), and further that the magnetic field and neutral pressure values were such that $\Omega_i/\nu_i \gg 1$ and that $\Omega_e/\nu_e \gg 1$. Then using the above conditions the electron and ion motion can be considered.

A. The Electron Motion

From equation (2), zero order conditions give:

$$v^o_{ex} = v^o_{ez} = 0 \quad ; \quad \text{and} \quad v^o_{ey} = -\frac{k_y \kappa ckT_e}{eH} \tag{4}$$

where $\kappa = \frac{1}{n_0}\left(\frac{dn_0}{dx}\right)$, and the 'o' superscript refers to zero order conditions.

First order equations from the x, y and z components of equation (2) relate the perturbed velocities v^1_{ex}, v^1_{ey}, and v^1_{ez} with the perturbed density n^1 and potential φ^1. These are:

$$v^1_{ex} = i\frac{e\nu_e}{m} k_x \varphi^1 - \frac{T_e}{m}\nu_e i\{k_x - \kappa\}\left(\frac{n^1_e}{n_0}\right) - \Omega_e v^1_{ey} \tag{5}$$

$$v^1_{ey} = i\frac{e\nu_e}{m} k_y \varphi^1 - i\frac{T_e}{m}k_y\left(\frac{n^1_e}{n_0}\right) + \Omega_e v^1_{ex} \tag{6}$$

$$v^1_{ez} = i\frac{e\nu_e}{m} k_z \varphi^1 - i\frac{T_e}{m}k_z\left(\frac{n^1_e}{n_0}\right) \tag{7}$$

Substituting these values in the equation of continutiy for electrons
there results a relationship between n^1 and φ^1 which is:

$$\left(\frac{n_e^1}{n_0}\right) = \frac{[k_z^2 - i\,\nu_e k_y \kappa/\Omega_e]}{[D_e k_z^2 - i\omega]} \frac{e}{m\nu_e}\,\varphi^1 \tag{8}$$

where $D_e = T_e/\nu_e m$ is the diffusion coefficient for electrons.

B. The Ion Motion

In a similar manner the ion equation of motion can be linearized
to obtain expressions for v_{ix}^1, v_{iy}^1, and v_{iz}^1. Then, substituting
these values into the continuity equation (1) for ions, the following
expression relating n^1 and φ^1 is obtained:

$$\left(\frac{n_i^1}{n_0}\right) = \frac{ck_y \kappa}{\omega H}\,\varphi^1 - \frac{k_\perp^2}{\omega \Omega_i^2}\,(\omega + i\nu_i)\,\frac{e\varphi^1}{M_i} \tag{9}$$

where $k_\perp^2 = k_x^2 + k_y^2$.

C. The Dispersion Equation

In the low frequency limit $(\omega \ll \Omega_i)$, and assuming quasi-
neutrality (i.e $n_i = n_e$), by combining equations (8) and (9) the dis-
persion equation relating ω and k can be obtained. This results
in the equation:

$$\omega^2 + i\omega[\omega_s + D_e k_z^2 + \nu_i] - i\omega_s \omega^* - D_e k_z^2 \nu_i = 0 \tag{10}$$

where the drift frequency $\omega^* = -k_y \left(\dfrac{cT_e \kappa}{eH}\right)$, and $\omega_s = k_z^2 \Omega_e \Omega_i / k_\perp^2 \nu_e$.
The above quadratic dispersion equation can be solved, and expressions
obtained for the $Re(\omega)$, and the growth rate $Im(\omega)$, versus k_z the
axial wavenumber. Substituting the values for the particular condi-
tions that prevail in the experiment, the dispersion equation can be
computed in each case. Some of these are shown in Figs.7-10.

However, in the approximation that k_z is large the $Re(\omega)$ tends to ω^*, and for $k_z \to 0$, it can be shown that $Re(\omega) \to 0$.

3. EXPERIMENTAL DETAILS

A. Apparatus

A schematic diagram of the apparatus used is shown in Fig.1. A uniform magnetic field is produced in a long solenoid formed by a series of coils each spaced 10cm apart, producing a uniform magnetic field ($\sim 0 \cdot 5\%$) in the volume of the plasma over a length of 200 cm. This field could be varied over the range $0 \cdot 1 - 3 \cdot 2$ kG. The plasma tube was aligned along the axis of the coils and was usually of borosilicate glass, although for some more critical diagnostic measurements, a silica tube was used, as mentioned later in Sec.3B. Two different diameter tubes were employed in order than the density gradient scale length could be varied; these were $2 \cdot 5$ cm and $5 \cdot 0$ cm. dia. Neutral gas (hydrogen or helium) was admitted to the tube through an inlet at one end and was allowed to flow through continuously during the course of an experiment. The gas pressure in the tube was monitored by Pirani gauges which were calibrated for the gas in use by means of a McLeod gauge. A combination of leak valve on the inlet side and variable baffle valve on the vacuum pump enabled fine control of the working pressure to be achieved. A variable length of plasma was selected by using a moveable anode which slid along the tube and was of finely gridded construction so that it did not impede the neutral gas inflow.

The plasma was formed in two ways. In the first case, a pulsed hot cathode technique was employed. At one end of the tube a small coiled tungsten cathode was supported, and this was coated with

lanthanum hexaboride to increase electron emission and reduce sputtering. This cathode was connected to earth through a small value resistor (typical value ~ 1 kΩ), and was heated from a half-wave rectified power supply (50 Hz) such that current was only flowing for one half cycle each period. During the off period, when no current was flowing in the cathode, a highly negative (- 500 V) going short pulse (duration 100 μsec) was applied to the cathode (with the anode earthed) thus producing a short burst of electrons which ionized the background gas. The plasma so formed then decayed exponentially for the duration of the "quiescent" period (some 9-10 msec).

The alternative method of plasma production used was a 'pulsed-off RF' excited plasma formed between metal straps around the tube and the end plates. This was tried to see if the presence of a hot cathode in the tube was generating undesirable effects, (such as 'hot' electrons, longitudinal electric fields, etc.) which might be the cause of the instability in this apparatus. As will be shown in Sec.4 there was no difference in the dispersion curve obtained by this production technique over that obtained when using the hot cathode method. The outline of this RF excitation method is shown dotted in Fig.1.

B. Diagnostic Techniques

(i) Probes

At the centre of the containing tube were two ports, 180° apart, and at one quarter the tube length was another pair at 90° apart azimuthally. Interchangeable probes could be inserted at each of these ports, and were moveable so that they could be set in any radial position. The cylindrical probes were constructed either of 1·0 mm or 0·125 mm diam tungsten wire sheathed in glass except for a 2·0 or 3·0 mm bare length at the end.

A longitudinally moveable probe was inserted from the cathode end, and could be moved over two thirds the length of the tube. This was constructed of a central insulated wire supported inside a 1·5 mm diam stainless steel tube, which itself was sheathed inside a glass tube of slightly larger diam. The tip of the probe was formed at 90° to the body by a tungsten wire (0·125 mm diam) sealed through the glass tube with its tip position at $a/2$. (a is the radius of tube.) Another probe similarly constructed was mounted directly at the periphery of the moveable anode and could therefore be rotated through the full 360° in order to detect the azimuthal variation of the instability.

Since the plasma under investigation was an afterglow of limited duration, and it was necessary to make fairly accurate time resolved measurements in the decay, it was essential that all these probes should have a short electrical time constant associated with them, and to this end the capcitance of the probes and associated leads were kept to a minimum. This was particularly so in the case of very small area probes where the small current drawn necessitates the use of relatively high resistors in the probe circuits. Typically, a time constant of 10^{-5} sec was obtained for 100 kΩ load resistor.

(ii) UHF Cavity

On the tube was mounted a cylindrical cavity (~ 15 cm diam, 10 cm long) operating in the TM_{010} mode (see Fig.1). At each end of the cavity were placed short cylinders, (~ 4 cm long) closely fitting the plasma tube, which acted at waveguides beyond cut-off at the resonant frequency ≈ 1350 MHz. The cavity was made from a solid block of brass which was split longitudinally and then the two halves were bolted together in position on the plasma tube. This procedure

eliminated any joins in the metal walls running across the direction of current flow for the particular made of oscillation. The smaller plasma tube was made of silica in order to reduce electrical losses at the microwave frequency, and thus enabled a Q value of ~ 5,000 to be achieved. The larger diameter tube was made of borosilicate glass with inferior electrical properties and also a thicker wall, and a Q value of only 1500-2000 was obtained. The cavity was used in its transmission mode, by feeding into a coupling loop on one side of the cavity, a signal from a Rohde and Schwarz generator (950-1900 MHz). The output was taken from a similar coupling loop in the opposite wall of the cavity, rectified by a crystal detector and fed to the oscilloscope input. Maximum power transmission was observed at resonance, and the power level was adjusted to the minimum necessary for observation. The frequency of the oscillation was measured using a Hewlett-Packard type 5245 counter (with 300-3000 MHz converter) to an accuracy of 3 parts in 10^9. Thus, the measurement of frequency differences which the method requires is reduced to the short-term stability of the signal generator which was of the order of 1 part in 10^5. The cavity was used either for accurate measurement of the average density, or alternatively, to estimate the electron collision frequency.

To measure the density the resonant frequency of the cavity without plasma present was first measured (f_0). The oscillator was then reset to a new frequency corresponding to a cavity resonance when a plasma of average density $\bar{n}_t$ was present. Then as the afterglow decayed from its starting density n_0, at some time t it passed through the given value of the density $\bar{n}_t$ and the detected output from the cavity showed a transmitted peak. The change in frequency

- 9 -

Δf corresponding to a change in average density, has been computed by a perturbation analysis method for values of $f_0 < f_p$, (where $f_p = (4\pi \, n(t) e^2/m)^{1/2}$ is the plasma frequency for that particular density $n(t)$). This analysis led to a relationship of the form[13].

$$\frac{\Delta f}{f_0} = F_r \left(\frac{r_1}{r_2}\right)^2 \left(\frac{f_p}{f_0}\right)^2 \tag{11}$$

where F_r is a form factor dependent on the geometry of the cavity and plasma; and r_1 and r_2 the radii of the plasma and cavity respectively. Curves of this function, F_r, are shown in the paper of Agder and Enander[13] for the various cavity modes of oscillation and so with its knowledge $n(t) (\propto f_p^2)$ can be obtained.

If losses in the plasma are taken into account by including a collision frequency ν_e for the electrons, the change in Q value of the cavity with and without the plasma present can be written[10] as

$$\frac{1}{Q} - \frac{1}{Q_0} = \frac{\nu_e \Delta f}{\pi \, f_0^2}$$

or alternatively

$$\nu_e = \frac{\pi \, f_0^2 \, \Delta(1/Q)}{\Delta f} \tag{12}$$

where Q_0 is the unloaded Q value of the cavity. Hence measurements of the change in Q of the cavity together with the frequency difference can lead to a value for ν_e.

4. RESULTS

A. Zero-Order Measurements

As was mentioned in Sec.3, the density was determined using the UHF cavity method, but this technique only allowed a determination of the mean density averaged over the cross-section of the plasma. Consequently, in order to determine the density profile across a radius

of the column, a single probe technique was used. The ion saturation
current $i_s(r)(\alpha \, n(r))$ to the single probe was measured at a fixed
time τ in the afterglow as a function of radial position. A typi-
cal profile for the larger tube is shown in Fig.2(a) taken in a H_2
plasma at a neutral pressure of 17 μ Hg, axial magnetic field
H = 175G and a time 2 msec in the afterglow. It is seen that the
inverse scale length, in this case $\kappa = \dfrac{1}{n_0} \left(\dfrac{dn_0}{dr} \right) \approx 1 \cdot 3 \pm 0 \cdot 1 \ \mathrm{cm}^{-1}$, is
constant over the radial range $1 \cdot 3 - 2 \cdot 5$ cm. It was checked that
similar reduced density profiles were obtained for various times
$\tau > 1$ msec in the afterglow, and at various positions along the plasma.
Also, as the length of the volume was varied similar profiles were
measured.

The electron temperature T_e and ion temperature T_i are
extremely difficult parameters to measure, and at first sight it
might be supposed that these temperatures could be assumed as ambient,
but a close study of the literature reveals that although this should
be true for the ions, the evidence suggests that elevated electron
temperatures can exist for several milliseconds into the afterglow[14-17].
Some effort has been expended on this measurement using a single probe.
However, the use of probes in low-density plasmas in a magnetic field
presents some difficulty, a discussion of which is given by Chen[18].
Fortunately, the temperature is one measurement which is least dis-
turbed under these conditions, provided that conditions for making
a valid probe measurement are appreciated. These are that the current
drain must be kept to an absolute minimum whilst a short enough response
time of the probe is retained. The drain problem is a serious
one and inevitably eventually affects the characteristic as the current
is taken nearer to the electron saturation value. This limits the

portion of the probe characteristic which is useful, to that part from the ion saturation current to some limiting value of electron current well short of saturation. This part of the curve represents electron current drawn mainly from the high-energy tail and thus electron temperatures based on the concept that the electron velocity distribution is Maxwellian would be in error if this condition was not satisfied. Similar reasoning applies to the use of an equal area double probe which in all cases sample this portion of the probe characteristic. However unless one supposes a unique combination of parameters changing in the appropriate manner to achieve the same effect, the fact that a nearly constant frequency with time is observed experimentally suggests that the temperature does not change rapidly during this period (i.e. from 2-6 msec after start of the decay). Measured temperatures within this period gave values between $800^{\rm O}$ and $1200^{\rm O}$K and thus, a value of $1000^{\rm O}$K was taken for calculation purposes. A typical semi logarithmic plot of electron current I_e against applied potential V_p is shown in Fig.3.

The measurement of electron-neutral collision frequency ν_e was made possible by noting the change in Q of a resonant cavity. This cavity, basically designed to measure the electron density, had a Q of 5000 when used with a silica discharge tube. Two possible methods were available as follows:

(i) To measure the change in Q produced as the resonant frequency with the plasma present was varied from $\Delta f = 0$ up towards the plasma frequency ω_p where collisional effects increased. This is the method outlined in Sec.3.

(ii) To use a fixed offset frequency, and measure the change $\Delta(1/Q)$ as a function of neutral pressure p. This should give a linear

relationship, and when the Q has been reduced to a small fraction
of its initial value gives a reliable result.

Both methods have been used and give good agreement. A plot of
$\Delta(1/Q)$ versus pressure is shown in Fig.4(a) for a hydrogen plasma
and in Fig.4(b) for a helium plasma. It is assumed that the measured
electron collision frequency is indeed the electron neutral collision
frequency since $\Delta(1/Q)$ is in fact linearly proportional to the
neutral pressure over a reasonable range of pressure. The final
values of (a) $\nu_e/p = 0 \cdot 70 \pm 0 \cdot 15 \times 10^9$ sec^{-1} for the hydrogen
plasma and (b) $\nu_p = 0 \cdot 80 \pm 0 \cdot 15 \times 10^9$ sec^{-1} for the He plasma
were adopted as those to be used in calculating a theoretical compari-
son with experiment.

The ion–neutral collision frequency ν_i proved to be an extremely
difficult parameter to measure, and as a consequence, its value was
estimated from theoretical comparison with the measured electron-
neutral collision frequency ν_e. From simple kinetic theory consider-
ations, the ratio of the collision frequencies ν_e/ν_i can be related
to the collision cross-sections S_i and S_e and their collisional
velocities v_i and v_e (where v_i and v_e are the thermal veloci-
ties of ions and electrons respectively) The relationship is
$\nu_e/\nu_i = v_i S_i/v_e S_e$. On the solid sphere approximation, if the ion dia-
meter is assumed to be much greater than the electron diameter, and
of the same order as the neutral particle diameter, $S_i/S_e \approx 4$. Hence
from a knowledge of the electron and ion temperatures T_e and T_i
respectively, the ion collision frequency can be obtained. This gave
(a) $\nu_i/p = 1 \cdot 0 \pm 0 \cdot 15 \times 10^6$ sec^{-1} for the He plasma and
(b) $\nu_i/p = 1 \cdot 5 \pm 0 \cdot 15 \times 10^6$ sec^{-1} for the hydrogen plasma.

B. Instability Measurements

The instability was observed as a decaying sinusoidal oscillation from a single probe in the plasma when the magnetic field and neutral gas pressure had been optimized. A typical oscillating decay signal is shown in Fig.5 where the output from two single probes separated azimuthally by 180° are presented. The properties of the oscillation were found as follows:

(i) Azimuthal Variation

The azimuthal variation in phase was observed by comparing the phase of the signal from the rotatable probe with that of one of the fixed probes. The amplitude was also measured on this rotatable probe. The azimuthal and amplitude variations were consistent with an azimuthal propagating wave, with either an $m = +1$, or $m = +2$ mode. Each was observed separately under different conditions.

(ii) Radial Variation

The variation in amplitude and phase was, again, measured on a radially moveable single probe. The smallest of the available probes was used in order to minimize any disturbance of the plasma, although the use of a large probe made no apparent difference. The resulting amplitude and phase variation was consistent with a $m = +1$ or $m = +2$ propagating wave, under the appropriate conditions for either mode. A plot of (b) the amplitude variation and (c) the phase variation for an $m = +1$ mode as a function of radius, is shown in Fig.2. This was taken, also, in the hydrogen plasma at $H = 175$ G and $p = 17 \ \mu$ Hg pressure.

(iii) Longitudinal Variation

The longitudinal variation of amplitude and phase was observed using the axially moveable probe. This was checked at various plasma

lengths, obtained by moving the position of the anode. Typical results are shown in Fig.6 for (a) the amplitude, and (b) the phase taken over a plasma length of 120 cm. The deduction from these results is that the basic configuration in the tube is a standing wave in the axial direction, with a wavelength approximately equal to the plasma length. This is in contrast to other drift-wave experiments[5] where one half-wavelength in the tube has been observed.

(iv)   The Dispersion Relationship

The frequency of the instability at any plasma column length was determined from oscilloscope display photographs of the decaying signal, as shown in Fig.5. By displaying the output from two probes 180° apart, a constant check can be kept that the mode number is constant. This procedure was adopted as the plasma length was varied, consequently allowing a ω-k dispersion diagram to be obtained. Experiments were first performed using the small diameter tube and the hot cathode plasma production technique. The magnetic field and neutral pressure were varied until optimum values were obtained. These conditions were then maintained constant throughout a series of experiments. Typical results are shown in Fig.7 for experiments performed in a helium plasma at the magnetic fields of (a) H = 500G and (b) H = 350G. Results obtained using a hydrogen plasma are shown in Fig.8 for the same magnetic fields.

As a check to obviate any effect due to the presence of the hot cathode in the plasma tube, a discharge was struck using a 27 MHz RF oscillator to produce the plasma. The afterglow was produced by "pulsing-off" this oscillator for $\sim$ 20 msec. Very similar results were obtained as can be seen by comparing the results obtained by the differing plasmas in Fig.8.

As a further check, a larger diameter discharge tube was tried, as this approximately halved the radial scale length. Under these conditions with $H = 175G$ it was possible to obtain both $m = +1$ and $m = +2$ modes in the tube, separately, as the plasma length was varied. The results are shown in Fig.9 for a helium plasma, and in Fig.10 for a hydrogen plasma for (a) $m = +1$, and (b) $m = +2$ azimuthal modes.

In Figs.7-10 the solid line shows the theoretically computed $Re(\omega)$ against k_z curve using the theory developed in Sec.2, and refers to the left hand scale. The theoretical growth rate γ is shown as the dotted curve in the figures and refers to the right hand scale.

5. DISCUSSION AND CONCLUSIONS

In Sec.2 the stability conditions for an inhomogeneous plasma in a magnetic field were investigated using slab geometry. It was shown that if electron-neutral, as well as ion-neutral collisions were taken into account an instability could be present in the plasma at certain wavelengths. In order to compare the experimental results obtained on a cylindrical plasma column, with these theoretical predictions, certain qualifications have to be made. These are:

(i) The cylindrical case has been approximated by taking over the cartesian coordinate calculation by assuming that $x \to r$, $y \to r\theta$, and $z \to z$. In this way $k_y \to m/r_0$ where r_0 is taken as the radius at which there is a maximum in the instability amplitude, and m is the azimuthal mode number associated with the mode. A condition for this approximation is that the azimuthal wave number k_y should be large compared with the inverse scale length κ. (i.e. $r_0\kappa/m \ll 1$). Experimentally, $r_0\kappa/m \approx 1$ is the worst case, and this is a point of

divergence between theory and experiment. However, recently Chu, Coppi, Hendel and Perkins[19] have performed a calculation for colli-sional drift waves in cylindrical geometry, and they comment that the dispersion relationship so obtained has almost the same form and coefficients as the 'local', slab model dispersion relationship. There-fore, it appears that, perhaps, this is not such an important point of divergence.

(ii)   The theory developed in Sec.2, is a small amplitude linearized theory, where the potential and density perturbations are assumed to be a small percentage of the zero-order values. In fact, any instabi-lity must have grown to an amplitude value which is limited by non-linear terms not included in the theory, and in this experiment values up to $n_1/n_0 \approx 25\%$ have been observed. However, some non-linear mechanisms[20,21] may limit the final instability amplitude so that the observed mode phenomena are closely related to the unstable perturba-tions predicted by the linear theory.

(iii)   Another important feature is that the slab model is based on the 'local' approximation. A more realistic calculation would be to evaluate the dispersion equation from the equations of motion in cylindrical geometry, with the appropriate boundary conditions taken into account. Then the solution to the eigenvalue problem could be used to examine the stability of the plasma. The 'local' approxima-tion can only be justified under the condition $\kappa r_0 \ll 1$. As mentioned previously, this is not the case experimentally.

(iv)   Other approximations involved are that $\nu_i/\Omega_i \ll 1$, and that $\nu_e/\Omega_e \ll 1$. Both these conditions are reasonably well satisfied, and their maximum value is $\approx 0 \cdot 3$ for both conditions in the helium plasma at 175G. Also, the low frequency approximation $\omega/\Omega_i \ll 1$ is

considered, and in this case the maximum value is ≈ 0.1. Consequently, this approximation is well satisfied.

(v)   In the calculation of the growth rate γ the larger quantities in the theory cancel leaving only smaller quantities with the consequence that $Im(\omega) = \gamma$ is subject to much larger error than the calculations for the $Re(\omega)$.

When the theoretical dispersion relationship for $Re(\omega)$ versus k_z is compared with the experimental results reasonably good agreement is obtained. The comparison is shown in Figs.7-10 where the full curve shows the numerically computed theoretical curve obtained by using the experimentally measured values for the zero-order parameters of the plasma. This good agreement is rather surprising in view of the approximations present in the theory and the possible errors present in the experimental results. The growth rate γ could not be measured directly, but its theoretically computed value is shown marked as the dotted curve in the figures, where its amplitude refers to the right hand scale. It should be noted that this vertical scale changes from one figure to the next, in order to obtain a convenient size plot. It is seen that for the $m = 1$ modes, in each case, that growth is predicted throughout the k_z range where oscillations were observed, although in some cases rather low growth rates were predicted (see Figs.7(a) and 8(a)). Also, the overlap between the predicted $m = + 1$ and $m = + 2$ growth rates shows that the $m = + 2$ mode should take over for a smaller k_z value, than that found experimentally. However, it was pointed out earlier that the predicted growth rates γ are subject to greater error than the $Re(\omega)$ values.

To conclude, the present results on the dependence of frequency ω and wave number k_z represent a comprehensive effort to identify

the observed instability. The measurements have been performed in both helium and hydrogen afterglow plasmas, at various field and neutral pressure values, and experiments have been performed in two plasma tubes in order to vary the radial density gradient. Comparison with the simple drift-dissipative theory in slab geometry shows reasonably good agreement. It would be desirable to compare the result with a theory calculated in full cylindrical geometry, including realistic boundary conditions. In spite of this, it is concluded that the observed instability is, indeed, the drift-dissipative instability.

REFERENCES

1   B.B. Kadomtsev, Plasma Turubulent, (Academic Press, N.Y., 1965).

2   A.B. Mikhailovski Rev. Plasma Phys. $\underline{3}$, 159 (1967). (Ed. M.A. Leontovich).

3   C.W. Hartmann and R.H. Munger, Proc. Conf. Phys. Quiescent Plasmas, Frascati (1967), p.181.

4   P.F. Little and P.J. Barratt, Proc. Conf. Phys. Quiescent Plasmas, Frascati (1967), p.173.

5   H.N. Hendel, T.K. Chu and P.A. Politzer, Phys. Fluids $\underline{11}$, 2426, (1968).

6   L. Enriques, A.M. Levine and G.B. Righetti, Plasma Phys. $\underline{10}$, 641, (1968).

7   R.V. Aldridge and B.E. Keen, Plasma Phys. $\underline{12}$, 1 (1970).

8   D.R. Pigache and G.N. Harding, Plasma Phys. $\underline{11}$, 805 (1969).

9   S.C. Brown and D.J. Rose, J. Appl. Phys. $\underline{23}$, 711 (1952).

10   S.J. Buchsbaum and S.C. Brown, Phys. Rev. $\underline{106}$, 196 (1957).

11   A.V.T. Timofeev Sov. Phys. - Tech. Phys. $\underline{8}$, 682 (1964).

12   A.V.T. Timofeev Sov. Phys. - Dokl. $\underline{8}$, 890 (1964).

13 B. Adgur and B. Enander, J. Appl. Phys. $\underline{33}$ 575 (1962).

14 R.L. Stenzel and R.W. Gould, Rev. Sci. Instr. $\underline{40}$, 1461 (1969).

15 D. Smith, C.V. Goodall and M.J. Copsey, J. Phys. (B), Atom. Mol. Phys. $\underline{1}$, 660 (1968).

16 E. Blue and J.E. Starks, J. Appl. Phys. $\underline{40}$, 4061 (1969).

17 B.T. Dodo, Plasma Phys. $\underline{11}$, 800 (1969).

18 F.F. Chen, Phys. Fluids $\underline{11}$, 811 (1968).

19 T.K. Chu, B. Coppi, H.W. Hendel and F.W. Perkins, Phys. Fluids $\underline{12}$, 203 (1969).

20 T. Stix, Phys. Fluids $\underline{12}$, 627 (1969).

21 T.H. Dupree, Bull. Am. Phys. Soc. $\underline{13}$, 263 (1968).
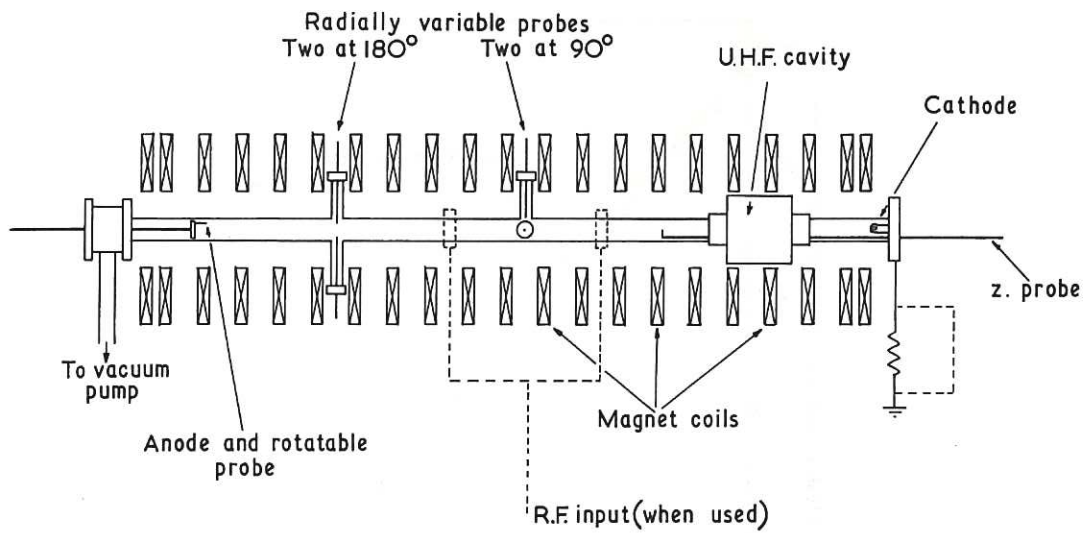
Fig.1 Schematic diagram of apparatus.
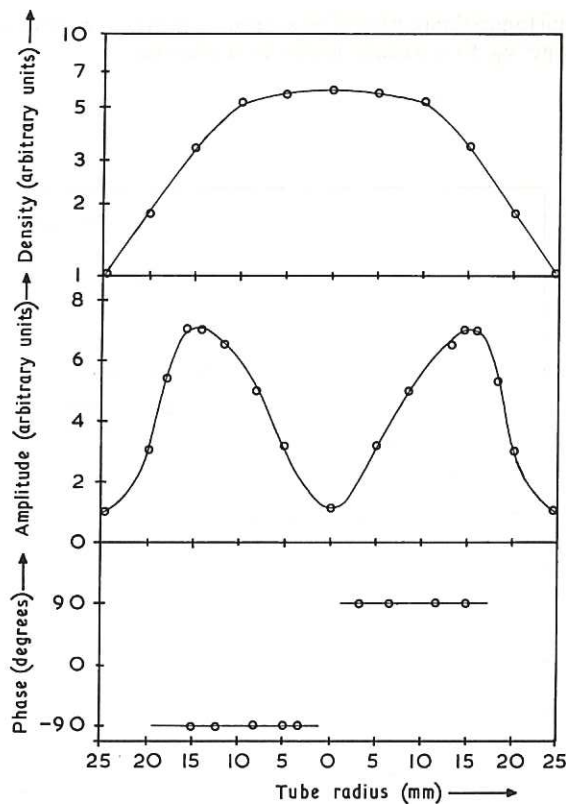
Fig.2 (a) Density profile, (b) amplitude variation, and (c) phase variation, as a function of radial position. These were taken from a hydrogen plasma in the larger diameter tube, in a magnetic field H = 175G and a neutral pressure of 17mTorr at a time of 2msec in the afterglow.   CLM-P 234
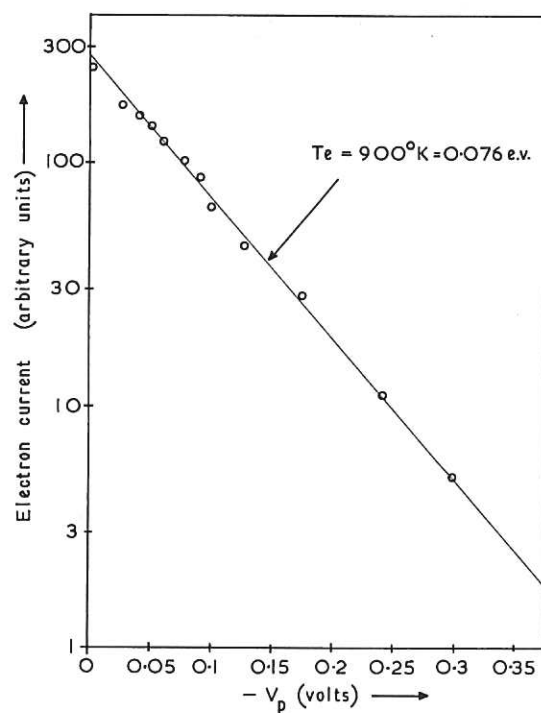
Fig.3 A semilogarithmic plot of electron current i_e versus applied voltage V_p to a single probe in a plasma.
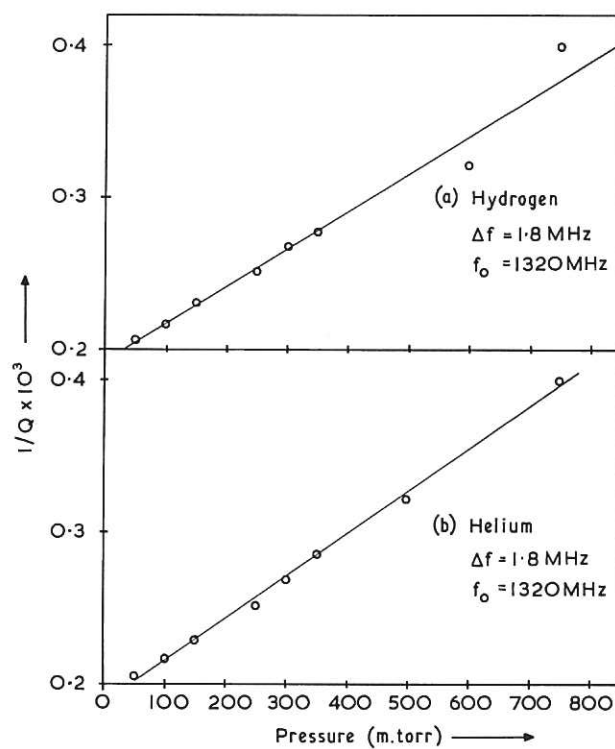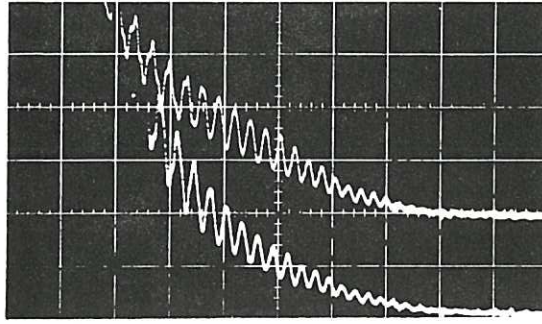

Fig.4 Change in 1/Q of the cavity as a fraction of neutral pressure for (a) a hydrogen plasma, and (b) a helium plasma.

Helium plasma   p = 20 m.torr

H = 500 gauss   m = +1

ω = 3 kHz

Horizontal scale   1 m.s./cm

Fig.5 Typical decay curves for the instability, showing the output from two single probes separated azimuthally by 180°.
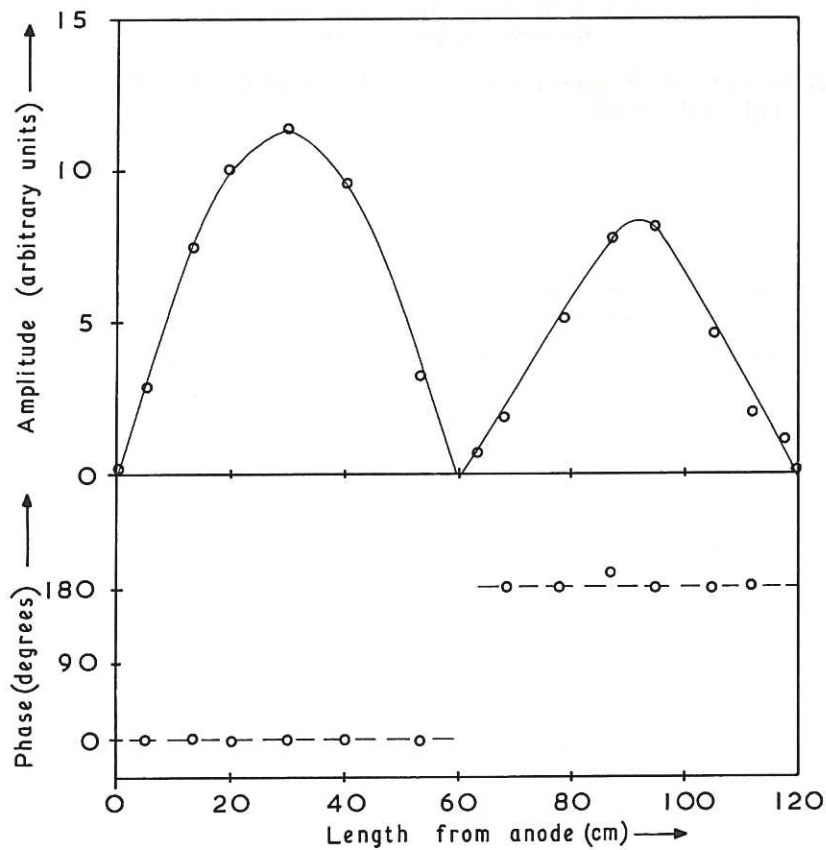

Fig.6 (a) The amplitude variation, and (b) the phase variation as a function of axial length, for a m = +1 azimuthal mode instability.   CLM-P 234
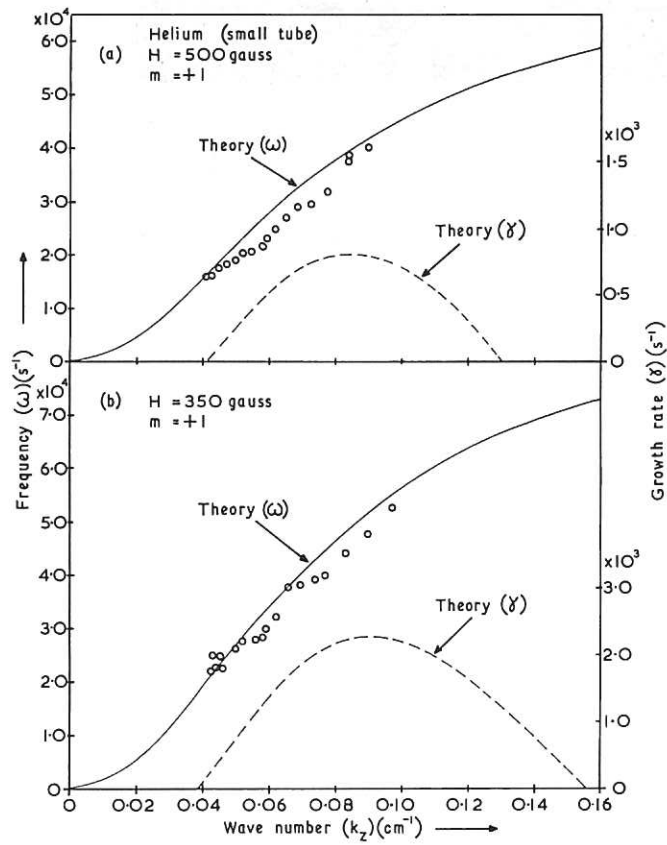
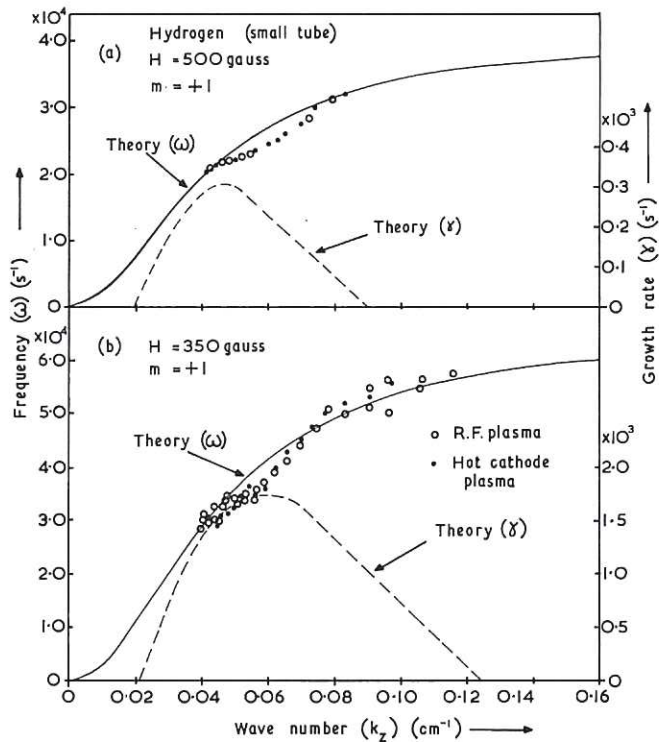Fig.7 Dispersion diagram for a helium plasma at (a) H = 500G and (b) H = 350G.

Fig.8 Dispersion diagram for a hydrogen plasma at (a) H = 500G and (b) H = 350G.

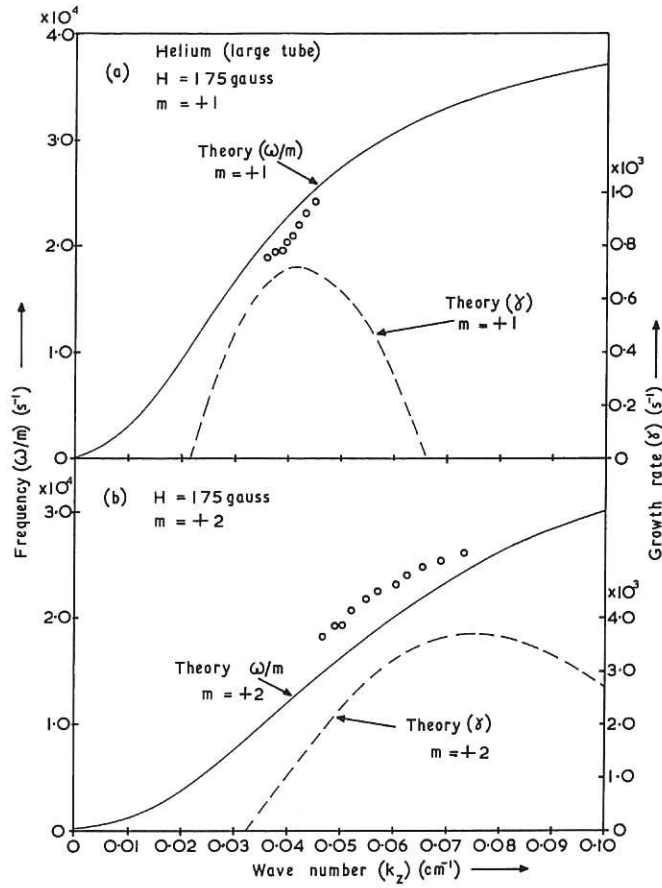Fig.9 Dispersion diagram for a helium plasma in H = 175G for
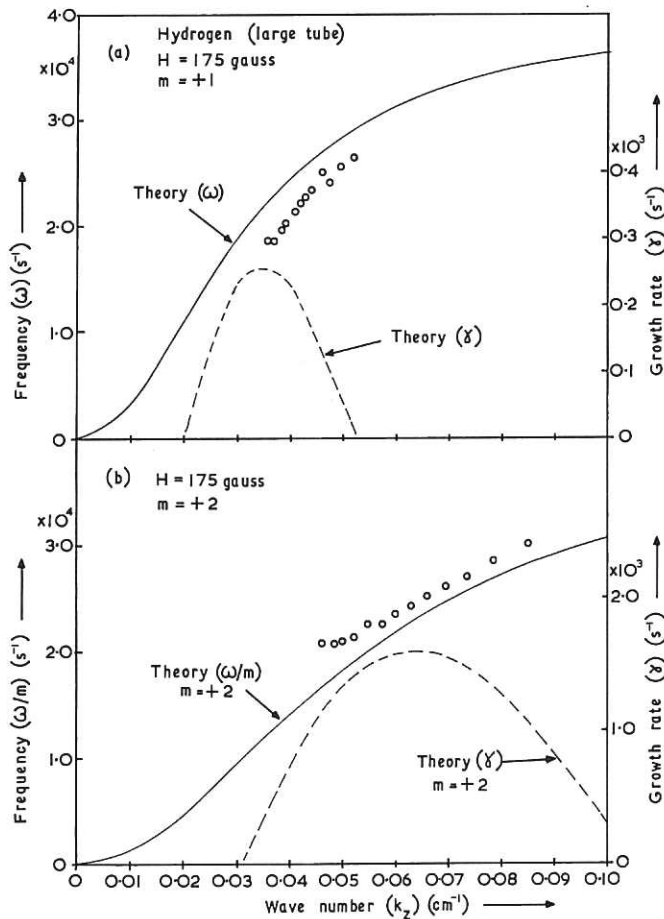(a) m = + 1, and (b) m = + 2 azimuthal mode number.

Fig.10 Dispersion diagram for a hydrogen plasma in H = 175G for
(a) m = + 1, and (b) m = + 2 azimuthal mode number.